Heliyon 11 (2025) e42051

Contents lists available at ScienceDirect

Heliyon

journal homepage: www.cell.com/heliyon

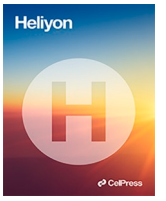

Research article

A single-cell transcriptome analysis reveals astrocyte heterogeneity and identifies CHI3L1 as a diagnostic biomarker in Parkinson's disease

Zhongying Gong *, Dan Guo, Yufeng Lin, Zhiwei Liu, Mengdi Lv, Xinxin Liu, Yang Yao, Sijia Wang, Yuan Wang, Zhiyun Wang **

Department of Neurology, Tianjin First Central Hospital, School of Medcine, Nankai University, Tianjin, 300192, China

ARTICLE INFO

Keywords:
Parkinson's disease
Astrocytes
CHI3L1
Inflammation
Diagnostic biomarker

ABSTRACT

Background: Parkinson's disease (PD) is the second most common neurodegenerative disease, characterized by motor and non-motor symptoms. It has been reported that astrocytes play a critical role in the pathogenesis and progression of PD. Here, we aimed to identify the heterogeneity of astrocytes and investigate genes associated with astrocyte differentiation trajectories in PD.

Methods: The single-cell transcriptomic profiles of PD samples were collected from the GEO database. We have identified subsets of astrocytes and analyzed their functions. The differentiation trajectory of astrocyte subtypes was explored using Monocle2. Inflammatory response scores were determined using AUCell. The levels of CHI3L1 mRNA and protein expressions in astrocytes were analyzed using qRT-PCR and Western Blot assay, respectively.

Results: We characterized seven cell types within the substantia nigra region of both PD and normal samples. Our analysis revealed that astrocytes comprised the second-highest proportion of cell types. Additionally, we identified three distinct subpopulations of astrocytes: Astro-C0, Astro-C1, and Astro-C2. Notably, Astro-C0 was associated with inflammatory signaling pathways. Trajectory analysis indicated that Astro-C0 occupies an intermediate stage of differentiation. The astrocyte-related gene CHI3L1 was found to be highly expressed in the Astro-C0 subpopulation. Furthermore, we observed increased levels of CHI3L1 mRNA and protein in LPS-induced astrocytes. Astrocytes exhibiting elevated CHI3L1 levels demonstrated interactions with microglia in PD patients. Lastly, we discovered that CHI3L1 was significantly overexpressed in PD patients and exhibited strong diagnostic potential for the disease.

Conclusion: This study clarified the heterogeneity of astrocytes in PD based on the single-cell transcriptomic profiles and found that CHI3L1 may be a diagnostic biomarker for PD.

* Corresponding author. Department of Neurology, Tianjin First Central Hospital, School of Medcine, Nankai University, No. 24 Fukang Road, Nankai District, Tianjin, 300192, China.

** Corresponding author. Department of Neurology, Tianjin First Central Hospital, School of Medcine, Nankai University, No. 24 Fukang Road, Nankai District, Tianjin, 300192, China.

E-mail addresses: 13212121250@163.com, 5020201054@nankai.edu.cn (Z. Gong), 13920760922@163.com, 5020201055@nankai.edu.cn (Z. Wang).

https://doi.org/10.1016/j.heliyon.2025.e42051
Received 18 August 2024; Received in revised form 15 January 2025; Accepted 15 January 2025
Available online 22 January 2025

Abbreviations:

PD	Parkinson's disease
GEO	Gene Expression Omnibus
ScRNA-seq	Single cell RNA sequencing
PCA	Principal component analysis
DEGs	Differentially expressed genes
GO	Gene Ontology
KEGG	Kyoto Encyclopedia of Genes and Genome
GSVA	Gene set enrichment analysis
WB	Western Blot
OPCs	Oligodendrocyte Progenitor Cells
NC	Normal Control

1. Introduction

Parkinson's disease (PD) is a prevalent neurological disorder. It is the second most common neurodegenerative disease characterized by motor and nonmotor symptoms [1]. Motor symptoms are classic findings of PD, including resting tremors, bradykinesia, postural instability, and rigidity [1,2]. The frequency of PD increases with age, and it affects 1 % of the population over the age of 60 [3]. The pathological features of PD are the presence of nerve inclusions in the form of Lewy bodies and Lewy neurons, and the loss of cells in the substantia nigra and other brain regions [4]. PD is defined as a synucleinopathy due to the significant presence of aggregated and misfolded α-synuclein species in Lewy bodies [4]. Currently, the therapy of PD is based on the control of motor symptoms by levodopa supplementation [1]. However, diagnosis of PD remains a challenge because the pathogenesis of PD is unknown, and diagnostic tests or biomarkers are still unable to make a definitive diagnosis from the earliest stages.

Previous studies have shown that neuroinflammation plays an important role in the etiology of neurodegeneration in PD [5,6]. Activated glial cells produce pro-inflammatory and neurotoxic factors causing neuronal damage and neurodegeneration [7,8]. It is well known that astrocytes are the most abundant glial cells in the central nervous system and surrounding neurons. Astrocytes protect neurons by releasing neurotrophic chemicals, producing antioxidants, and removing waste items, such as aggregated α-synuclein and damaged mitochondria [9,10]. In the brains of neurodegenerative disease patients, astrocytes migrate and become hypertrophic reactive astrocytes [11]. In PD, reactive astrocytes formed by inflammatory stimuli increase cytokine secretion such as IL-6 and RANTES [12]. Moreover, reactive astrocytes emit pro-inflammatory cytokines including TNF-α and IL-1β, causing neurotoxicity and neuronal death, which are associated with the pathogenesis of PD [13,14]. Liddelow et al. have discovered that activated microglia secrete IL-1α, TNF-α, and C1q, which induce neurotoxic A1 astrocytes that are detected in postmortem brains of PD patients [15]. Recent studies have revealed the regional heterogeneity of astrocytes [16,17]. However, the composition of the astrocyte subtypes in substantia nigra samples of PD and their interaction with other glial cells remains unclear.

In recent years, with the development of single cell sequencing technology, single-cell RNA sequencing (scRNA-seq) technology has enabled accurate and in-depth studies of intra- and inter-cell heterogeneity in neurodegenerative disease. Lang et al. have Lang et al. have reconstructed the PD disease progression process by single-cell transcriptome analysis of induced pluripotent stem cell dopamine neurons, identifying histone deacetylase 4 as a regulator of the Parkinson's cell phenotype [18]. Xu et al. have reported that abnormal changes occur in the composition and transcriptional status of immune cells in Alzheimer's disease, and Alzheimer's disease-specific clonotypes are enriched in T cell and B cell receptor [19]. Collectively, scRNA-seq is a powerful and unbiased tool for the analysis of heterogeneous and functional sub-populations. In this study, we collected the single-cell sequencing data of nigrostriatal samples with PD from the GEO database to identify the heterogeneity of astrocytes and investigate genes associated with astrocyte differentiation trajectories in PD. The present study reveals the heterogeneity of astrocytes and changes in the expression of specific genes in PD, which may provide molecular-level insights for the development of new therapeutic strategies.

2. Materials and methods

2.1. Study subjects

ScRNA-seq data of PD samples were collected from the Gene Expression Omnibus database (GEO, https://www.ncbi.nlm.nih.gov/geo/), including GSE148434, GSE157783, GSE140231, and GSE126836 datasets. GSE148434 included 6 normal substantia nigra samples and 6 substantia nigra samples from PD patients. GSE157783 contained 6 normal substantia nigra samples and 5 substantia nigra samples from PD patients. GSE140231 and GSE126836 had 6 and 6 normal substantia nigra samples, respectively.

Bulk RNA-seq data of PD samples with complete survival samples were downloaded from the GSE136666 (5 normal substantia nigra samples and 5 substantia nigra samples from PD patients), GSE114517 (6 normal substantia nigra samples and 17 substantia nigra samples from PD patients), and GSE148434 (6 normal substantia nigra samples and 8 substantia nigra samples from PD patients) datasets (Table S1). Moreover, whole blood RNA transcriptome (RNA-seq) sequencing data of 12 PD patients and 14 healthy control individuals were downloaded in the GSE165082 dataset.

2.2. ScRNA-seq data analysis and cluster annotation

The scRNA-seq data from PD and healthy samples were analyzed using Seurat (v4.1.1). Cells with mitochondrial content exceeding 20 %, hemoglobin content above 5 %, and gene expression levels below 500 or above 20, 000 were filtered out. Doublets in the scRNA-sequencing data were predicted using DoubletFinder to remove multicellularity from the dataset to ensure the reliability and accuracy of the results of subsequent analyses. The data were normalized using the default parameters of the "NormalizeData", 2000 highly variable genes were selected by the "FindVariableFeatures" function. These highly variable genes were then normalized using "ScaleData", and then principal component analysis (PCA) was performed using "RunPCA" function, and the top 20 principal components were retained for further analysis. The batch effects were corrected by "RunHarmony" with R-package harmony. The integrated data were again dimensionality and clustering based on the results of harmony (resolution 0.3). Cell subpopulations were annotated with the cellmark2.0 database based on the common cell mark gene.

2.3. Differential gene and enrichment analyses

The differentially expressed genes (DEGs) between PD and normal control (NC) groups were identified using FindMarkers in the Seurat package, according to the $|\text{Log2FC}|>0.3$ and p. adjust <0.05. The gene ontology (GO, including biological processes (BP), cellular component (CC), and molecular functionalities (MF)) and the Kyoto Encyclopedia of Genes and Genomes (KEGG) enrichment analyses were performed using R language ClusterProfiler [20], and the significantly enriched pathways were screened using $p < 0.05$.

2.4. Astrocyte subpopulation and gene set variation analysis (GSVA)

To identify astrocyte subpopulations, we integrated cells from different samples and selected the top 1000 genes with high variables in astrocytes. Additionally, we employed unsupervised clustering methods, specifically the Louvain algorithm, based on the top 20 principal components (PCs) of the integrated dataset, to delineate three distinct astrocyte subpopulations. The DEGs between astrocyte subpopulations were identified using FindAllMarkers, according to the $|\text{Log2FC}| > 1$ and p. adjust <0.05.

To investigate the functional network of DEGs among astrocyte subpopulations, we downloaded h. all:HALLMARK gene set from the MSigDB v2023.1 (https://www.gsea-msigdb.org). GSVA was applied to assess the differences in biological pathways between astrocyte subpopulations.

2.5. Trajectory analysis

The trajectory analysis was performed using the Monocle 2 v2.28.0 [21] package to reveal astrocyte differentiation trajectories. An integrated expression matrix, which accounted for the deletion of batch effects, served as the input data. Unit trajectories and evolutionary order were inferred utilizing the default parameters. The highly variable genes associated with cell trajectories were identified using the graph_test function.

2.6. Inflammatory response score

The genes in the PD astrocyte groups were evaluated for their inflammatory response using the R package AUCell v1.16.0 [19]. The inflammatory response score for each cell was determined by calculating the area under the curve (AUC) value for the set of inflammation-associated genes. UMAP plots were then colored according to these AUC scores. The gene set associated with the inflammatory response was obtained from the Gene Ontology (GO) term "inflammatory response" (GO: 0006954).

2.7. Intercellular communication

The CellChat (v1.5.0) package [22] was used to predict and visualize biologically significant intercellular communication. In brief, a CellChat object was made using the createCellChat function. The object was annotated with tags and overexpressed genes were identified, after which the computeCommunProb function was used to infer the communication probability, and the computeCommunProbPathway function was used to predict the intercellular communication for each cell signaling pathway.

2.8. Cell culture and constructing inflammation cell model

Mouse astrocytes (C8-D1A) were purchased from the cell bank of the Chinese Academy of Sciences (275,679, Shanghai, China). The cells were cultured in Dulbecco's modified Eagle medium (DMEM; Gibco, Grand Island, NY, USA) containing 1 % penicillin/streptomycin (Gibco) and 10 % fetal bovine serum (Invigentech). The cells were placed in a humidified incubator maintained at 37 °C with 5 % CO_2. Next, the C8-D1A cells were incubated with 1 μg/mL lipopolysaccharide (LPS, L8880, Solarbio) for 24 h to induce the inflammation cell model.

2.9. RT-qPCR

Total RNA was extracted from cells using the TRIzol (OSR-M610, TIANGEN). The quality and concentration of the extracted RNA

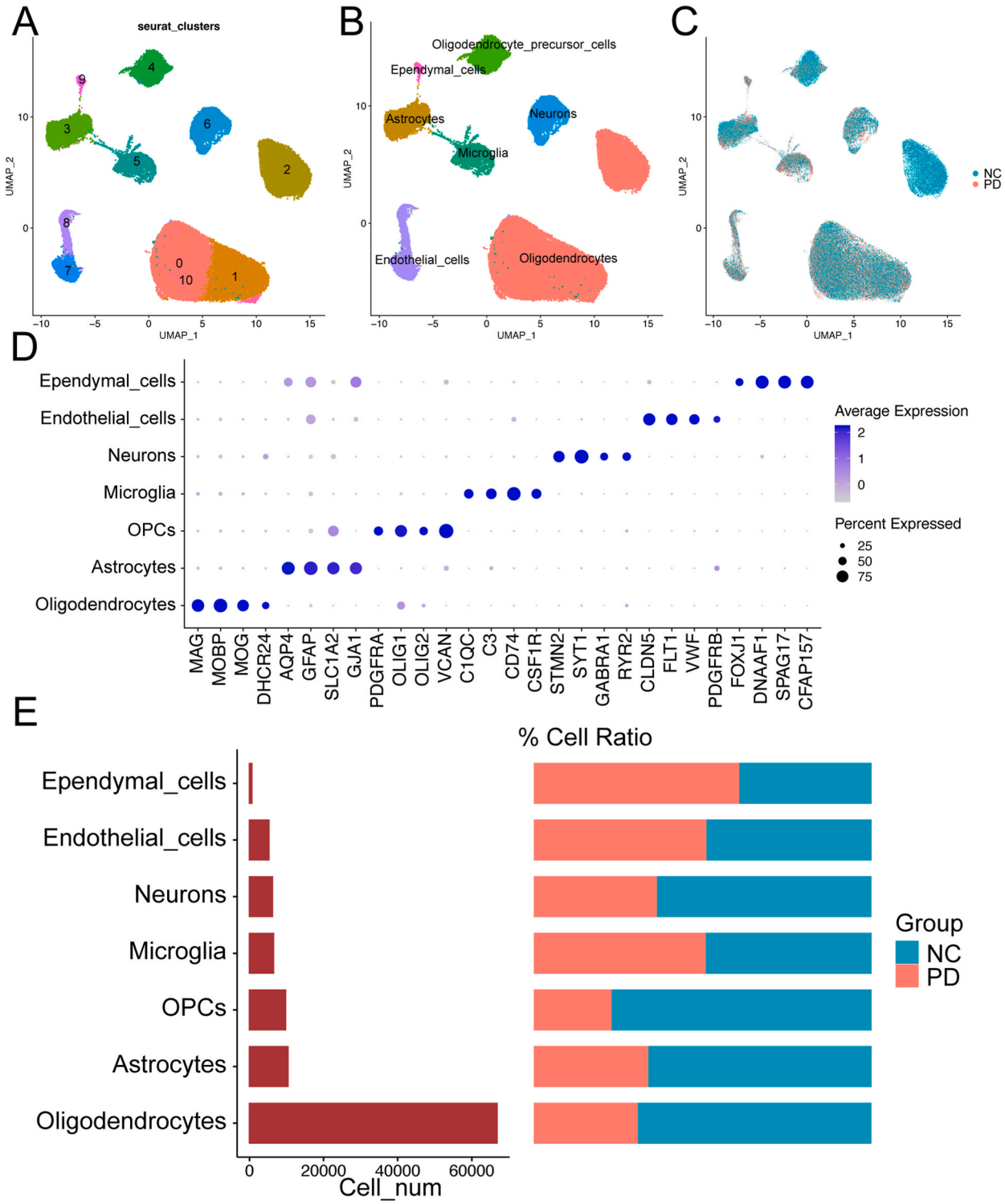

Fig. 1. ScRNA-seq data revealed distinct cellular constitutions in Parkinson's disease and normal control samples.
The UMAP plot of cells was color-coded by clusters (A) and cell type (B). C. The expression of marker genes of seven-cell types. D. The UMAP plot showed cell distribution in Parkinson's disease and normal control samples. E. The proportions of seven-cell types in PD and NC samples.

were assessed using a UV spectrophotometer. Reverse transcription was performed using the cDNA reverse transcription kit (KR118-02, TIANGEN). qPCR assay was conducted employing LightCycler 480 II Fluorescence Quantitative System (Roche, Basel, Switzerland). The reference gene was β-Actin, and the primer sequences were listed in Table S2. The mRNA expression levels were calculated according to the $2^{-\Delta\Delta CT}$ (three repeats).

2.10. Western Blot (WB)

The total protein was extracted from the cells using RIPA lysis solution (HY-K1001, MedChemExpress), and its concentration was

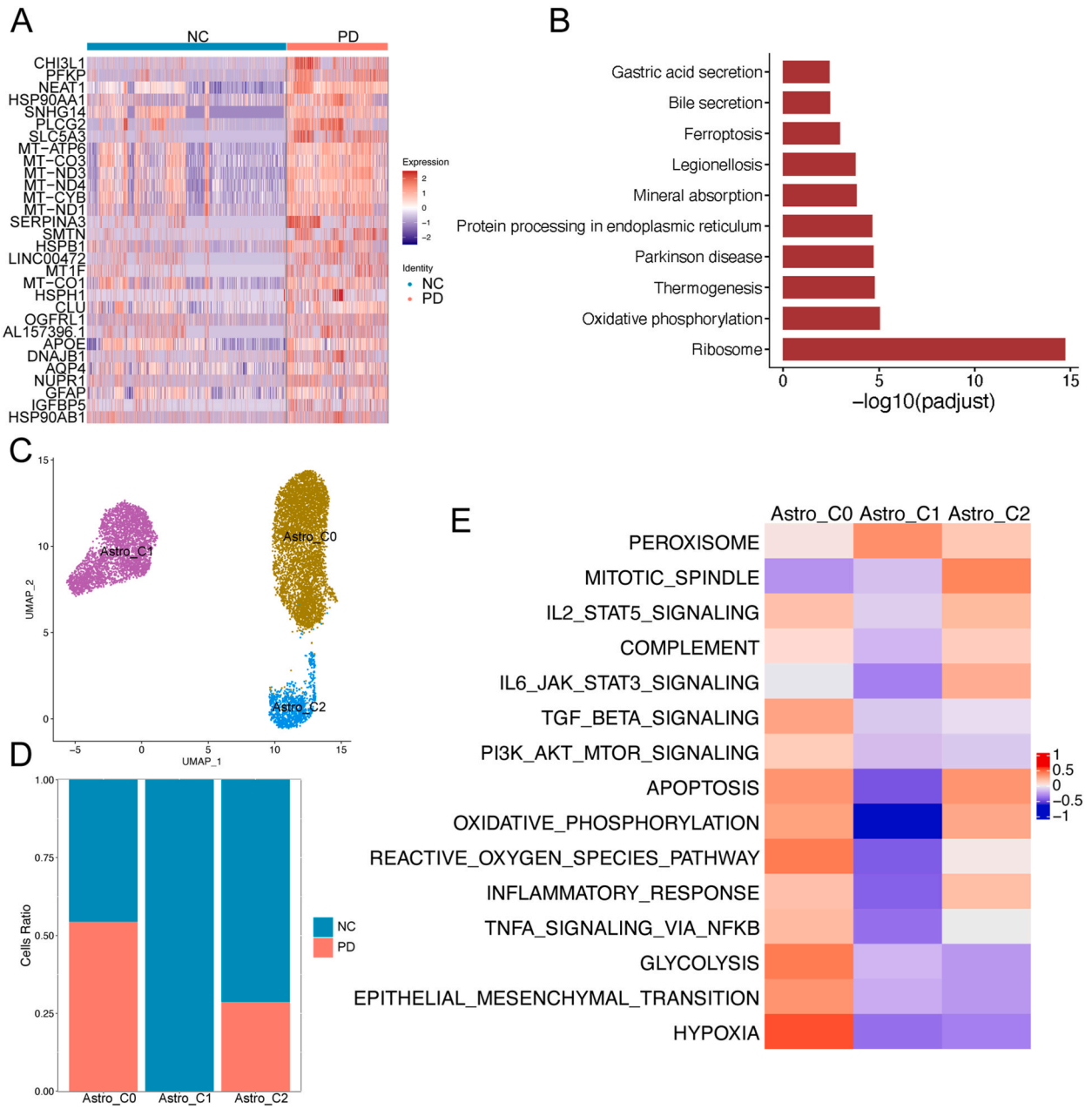

Fig. 2. Identification of astrocyte subpopulations in Parkinson's disease and normal control samples.
A. The differentially expressed genes (DEGs) in astrocytes between the Parkinson's disease and normal control groups. B. The result of Gene Ontology and Kyoto Encyclopedia of Genes and Genomes enrichment analyses. C. The UMAP plot of astrocyte subpopulations (Astro-C0, -C1, -C2). D. The proportion of astrocyte subpopulations in Parkinson's disease and normal control groups. E. The result of Gene set variation analysis for marker genes of astrocyte subpopulations.

determined using the Bradford Protein Quantification Kit (E161, Genstar). The internal reference used in the experiment was β-actin (AC026, abclonal) and the secondary antibody used was HRP Goat Anti-Rabbit IgG (H + L) (AS014, abclonal). The primary antibody used was *CHI3L1* antibody (12036-1-AP, proteintech), and the secondary antibody used was HRP Goat Anti-Rabbit IgG (H + L) (AS014, abclonal). The protein bands were detected using a Western blotting detection system (Tanon, Tanon 4800, Shanghai, China). The experimental results were analyzed using Image J software to determine optical density.

2.11. Statistical analysis

All experiments were conducted a minimum of three times. Data analysis and visualizations were performed using GraphPad Prism 10. Statistical significance was assessed by comparing mean values (±SD) using a student's *t*-test for independent groups and was expressed for *p < 0.05; **p < 0.01; ***p < 0.001.

3. Results

3.1. ScRNA-seq data revealed distinct cellular constitutions in PD and NC samples

Following quality control and filtration, a total of 34,671 cells from PD samples and 70,830 cells from NC samples were clustered into 11 cellular subpopulations using dimensionality reduction clustering analysis (Fig. 1A). Based on the expression of marker genes, these 11 cellular subpopulations were categorized into 7 cell types: ependymal cells (DANF1, SPAG1), endothelial cells (CLDN5, VWF), neurons (SYT1, STMN2), microglia (CD74, CSF1R), oligodendrocyte progenitor cells (OPCs, VPAN, OLIG1), astrocytes (AQP4, GFAP), and oligodendrocytes (MOBP, MOG) (Fig. 1B-C, Table S3). As illustrated in Fig. 1E, oligodendrocytes constituted the largest proportion of cells in the substantia nigra, followed by astrocytes (Fig. 1D-E).

3.2. Identification of astrocyte subpopulations in PD and NC samples

To further investigate the expression of genes in astrocytes between the PD and NC groups, we analyzed the DEGs between the two groups (Table S4). We found that *GFAP*, *AQP4*, *SERPINA3*, and *CHI3L1* were up-regulated in the PD group (Fig. 2A). The GO and KEGG enrichment analyses showed that the up-regulated DEGs were highly enriched in oxidative phosphorylation, PD, and ferroptosis signaling pathways (Fig. 2B).

To elucidate the detailed subpopulations of astrocytes and their roles in the PD, we performed the sub-clustering of astrocytes and obtained three astrocyte subpopulations: Astro-C0, -C1, -C2 (Fig. 2C–Table S5). Notably, the proportion of Astro-C1 subpopulations was all derived from NC samples (Fig. 2D). GSVA indicated that the Astro-C0 and -C2 subpopulations were associated with inflammation and apoptosis signaling pathways (Fig. 2E).

3.3. Pseudotime Trajectory Identified differentiation trajectory of astrocyte subtypes

Furthermore, we calculated the differentiation trajectory of three astrocyte subtypes (Fig. 3A) and organized the cells along a pseudotime trajectory. In this trajectory, the Astro-C1 subpopulation, which was present only in the NC group, clustered at the front end of the differentiation pathway, followed by a gradual activation into the Astro-C0 and Astro-C2 subpopulations. The distribution of PD cells varied along the activation trajectories of the astrocytes (Fig. 3B). To further characterize the molecular phenotypes of these two activated astrocyte states, we identified genes that correlated with the activity trajectories (Fig. 3B–Table S6).

In addition, we analyzed the expression of the top three genes associated with astrocyte activation trajectories. We discovered that *CHI3L1* was lowly expressed in the Astro-C1 (at the beginning of the pseudotime trajectory) and Astro-C2 (at the end of the pseudotime trajectory) subpopulations and highly expressed in the Astro-C0 (at the beginning of the pseudotime trajectory) (Fig. 3C-D).

3.4. *CHI3L1*^{High} astrocytes had a higher inflammatory response in PD patients

The astrocytes from 11 PD samples were divided into *CHI3L1*^{High} and *CHI3L1*^{Low} groups in the PD samples (Fig. 4A), and these two groups were distributed in both Astro-C0 and Astro-C2 subpopulations (Fig. 4B). Moreover, we identified DEGs between *CHI3L1*^{High} and *CHI3L1*^{Low} groups and found that astrocyte-related genes (*C3*, *BCL6*, *SERPINA3*, and *VEGFA*) were highly expressed in the *CHI3L1*^{High} group (Fig. 4C). The levels of inflammatory response score were significantly increased in the *CHI3L1*^{High} group compared to the *CHI3L1*^{Low} group (Fig. 4D-E, Table S7).

Furthermore, we constructed an astrocyte inflammation model using LPS and found that the expressions of C3, TNF-α, and IL-6 mRNA levels were elevated in the LPS-induced astrocyte groups compared to the NC group (Fig. 5A). Moreover, the levels of *CHI3L1* mRNA and protein were increased in the LPS-induced astrocyte groups (Fig. 5A and B, Fig.S1, Fig.S2, LPS vs. NC).

3.5. *CHI3L1*^{High} astrocytes had interactions with microglia in PD patients

To explore the interactions and signaling networks between *CHI3L1*^{High} and *CHI3L1*^{Low} astrocytes and other cells, we measured the expression of various ligand-receptor pairs (Table S8). Compared to *CHI3L1*^{High} astrocytes, the interaction between *CHI3L1*^{High} astrocytes and microglia was increased (Fig. 6A and B, Fig. S3A, S3B).

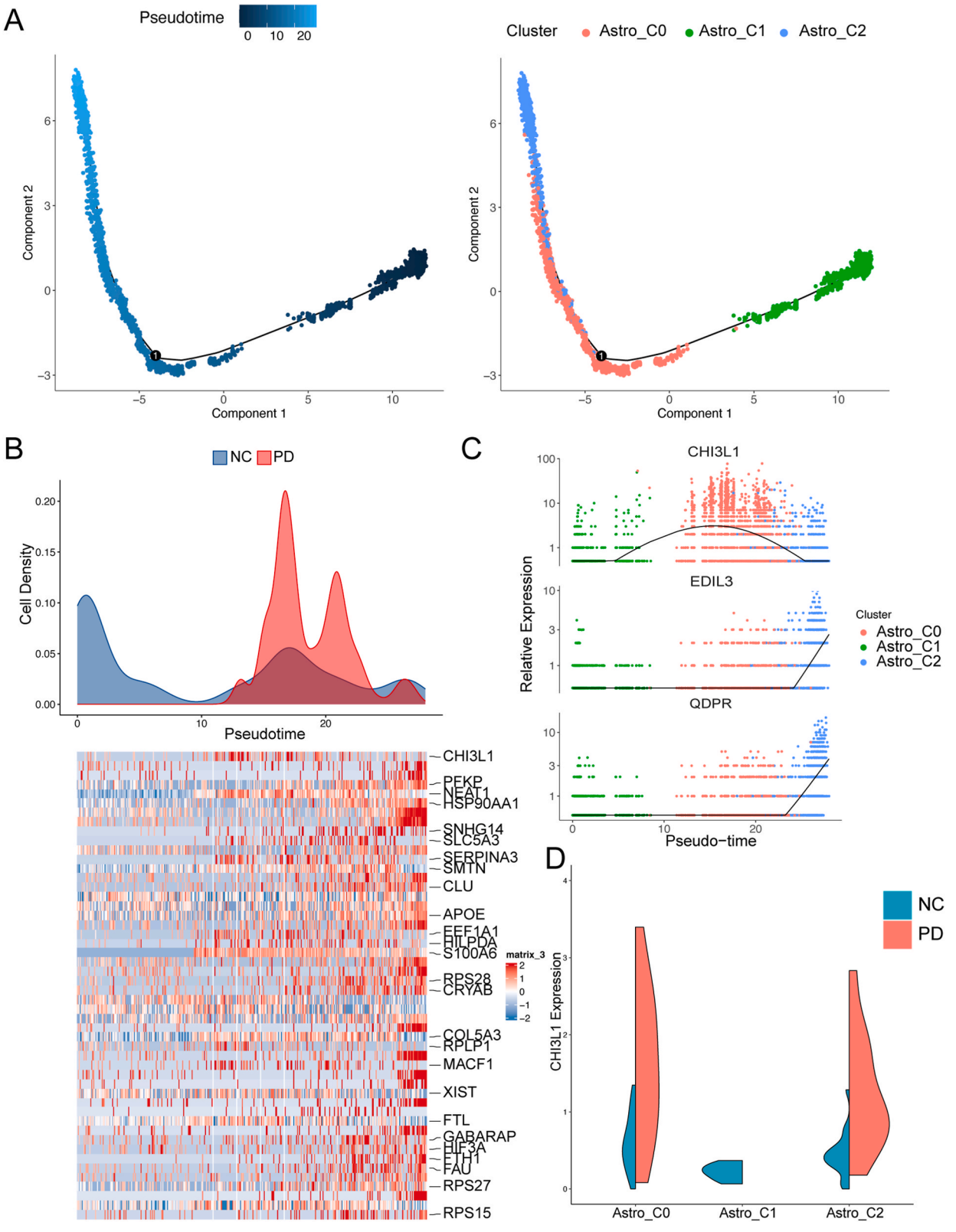

(caption on next page)

Fig. 3. Pseudotime Trajectory Identified differentiation trajectory of astrocyte subtypes.
A. The differentiation trajectory of three astrocyte subtypes. B. Cell density distribution along the timeline for Parkinson's disease and normal control samples (upper panel) and expression heatmap of 50 genes associated with astrocyte activation trajectories (lower panel). C. The expression of the top three genes associated with astrocyte activation trajectory. D. The expression of CHI3L1 in Astro-C0, -C1, -C2 in the Parkinson's disease and normal control groups.

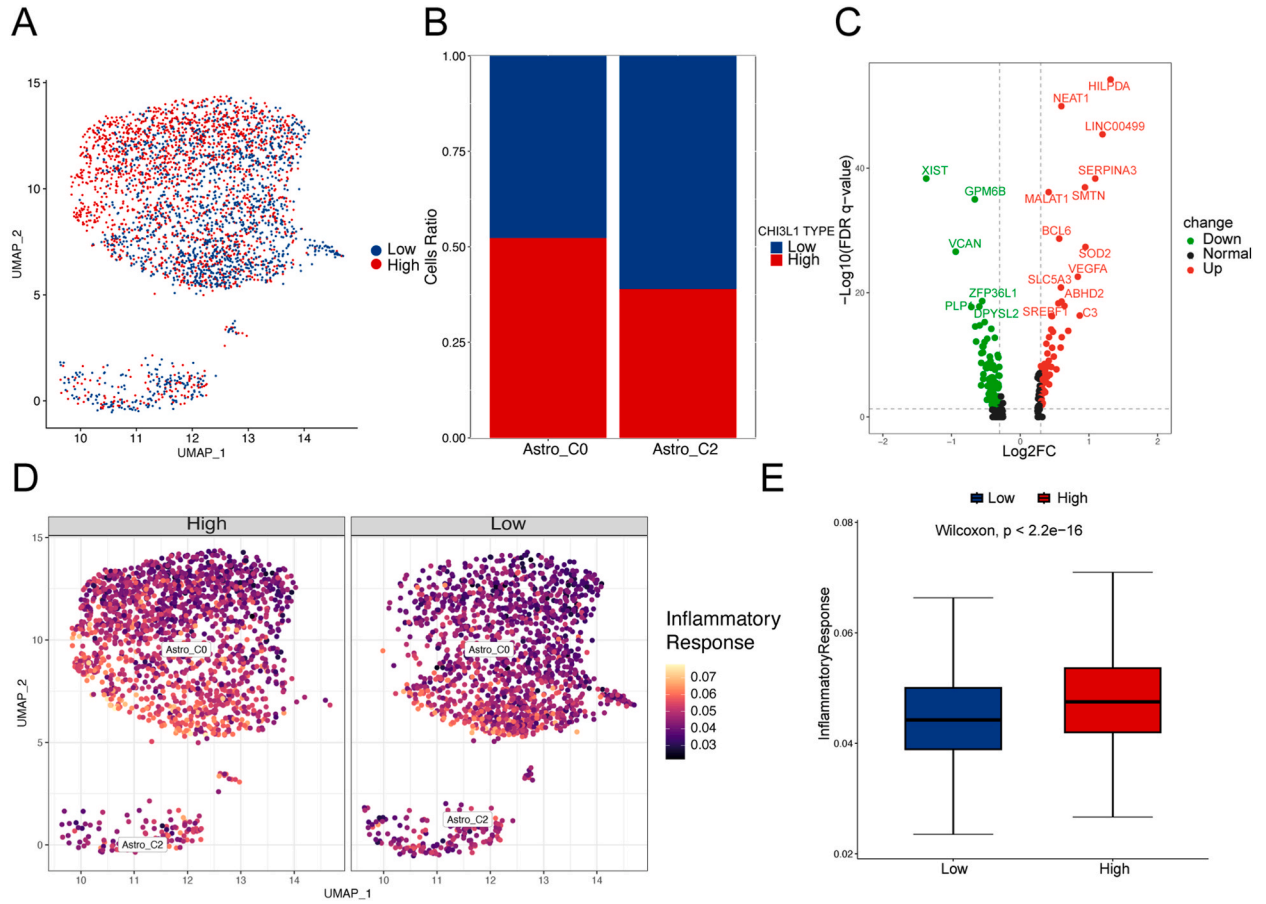

Fig. 4. *CHI3L1*^{High} astrocytes had a higher inflammatory response in Parkinson's disease **patients**.
A. Astrocytes were divided into *CHI3L1*^{High} and *CHI3L1*^{Low} groups in the Parkinson's disease samples. B. The proportion of *CHI3L1*^{High} and *CHI3L1*^{Low} astrocytes in Parkinson's disease samples. C. The differentially expressed genes between *CHI3L1*^{High} and *CHI3L1*^{Low} groups. D-E. The level of inflammatory response score in the *CHI3L1*^{High} and *CHI3L1*^{Low} astrocytes.

Furthermore, we analyzed receptor-ligand pairs (LRs) of *CHI3L1*^{High} and *CHI3L1*^{Low} astrocytes interacting with other cells and found that C3- (ITGAX + ITGB2), CSF1-CSF1R were present only in *CHI3L1*^{High} astrocyte-microglial cell interactions, FGF2-FGFR3 were present only in *CHI3L1*^{High} and *CHI3L1*^{Low} astrocyte interactions, and FGF2-FGFR2 were present only in astrocyte-oligodendrocyte interactions (Fig. 6C).

The LRs of *CHI3L1*^{High} astrocytes interacting with microglia involved two signaling pathways: CSF and COMPLEMENT (Fig. 6D and E). The CSF was a unique signaling pathway in CHI3L1^{High} astrocytes and microglia (Fig. 6D). *CHI3L1*^{High} and *CHI3L1*^{Low} astrocytes in the FGF signaling pathway had a stronger role (Fig. S4).

3.6. *CHI3L1 might be a marker for pre-diagnosis of PD*

Gene regulatory network analysis revealed that the expression of transcription factor (TF) was significantly different between *CHI3L1*^{High} and *CHI3L1*^{Low} astrocytes (Fig. S4). We analyzed the expression of *CHI3L1* in PD and NC samples from three bulk RNA-seq datasets, GSE136666, GSE114517, and GSE148434 (Fig. 7A–B,7D), and found that only in the GSE148434 dataset, *CHI3L1* was significantly overexpressed in PD samples. In the GSE136666 and GSE114517 datasets, PD patients had Braak stage 5–6, while in the GSE148434 dataset, PD patients had Braak stage 2–3. Moreover, we found that *CHI3L1* expression was higher in blood samples of PD patients compared to blood samples of healthy control individuals (Fig. 7C) in the GSE165082 dataset. Our previous analysis also

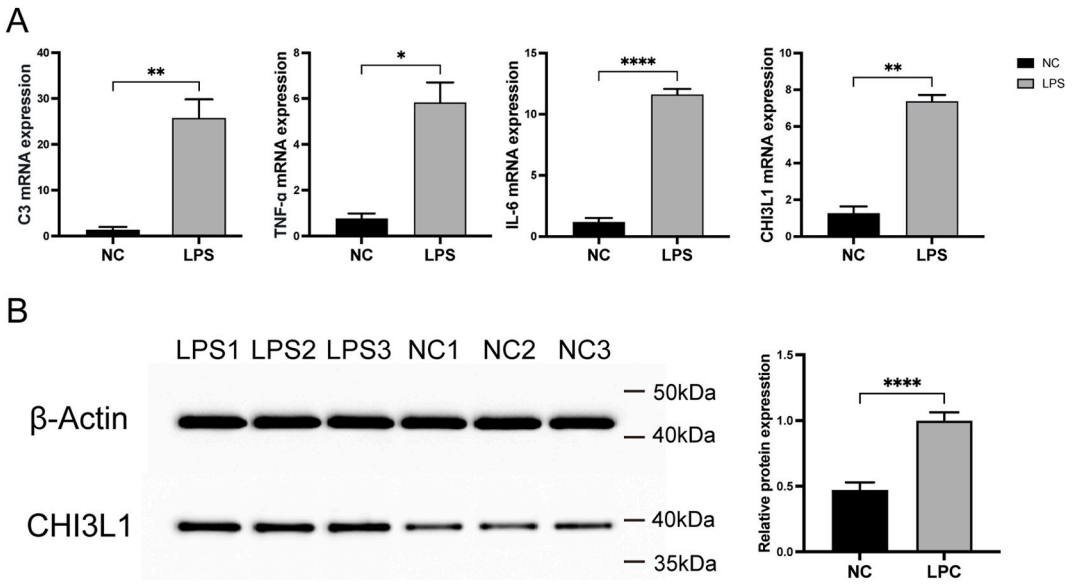

Fig. 5. The expression of *CHI3L1* was increased in the Lipopolysaccharide-induced astrocytes.
A. The expressions of C3, TNF-α, IL-6, and CHI3L1 mRNAs in the Lipopolysaccharide-induced astrocyte group were detected using qRT-PCR. B. The level of CHI3L1 protein in the Lipopolysaccharide-induced astrocyte group was measured by Western blot analysis. * means $p < 0.05$, ** means $p < 0.01$, *** means $p < 0.001$.

showed that *CHI3L1* expression was increased in the middle of the astrocyte differentiation trajectory (Fig. 3C). Moreover, in the GSE148434 dataset, we found that the area under the curve (AUC) of *CHI3L1* was 1 (Fig. 7E). These results indicated that *CHI3L1* might be used as a marker for pre-diagnosis of PD.

4. Discussion

PD is a progressive neurodegenerative condition pathologically defined by the loss of dopaminergic neurons in the substantia nigra and the development of protein inclusions known as Lewy bodies [23]. Multiple investigations of peripheral blood and cerebrospinal fluid from PD patients have revealed changes in inflammatory markers and immune cell populations that may trigger or worsen neuroinflammation and prolong the neurodegenerative process [24–26]. It has been demonstrated that astrocytic lesions were present in the substantia nigra and striatum of the brain in PD patients [23,27]. Therefore, studying astrocyte populations in the substantia nigra of PD patients will help us better understand the pathogenesis of PD.

In this study, we identified seven cell types in the substantia nigra of PD and healthy samples. Among these, oligodendrocytes were the most cell constitutions in the substantia nigra, followed by astrocytes. Oligodendrocytes and astrocytes are glial cells in the CNS. Fan et al. integrated high-quality scRNA-seq data and observed a decrease in oligodendrocytes and a significant increase in microglia in the midbrain of PD patients [28]. Smajić et al. also found that in the PD midbrain, the proportion of oligodendrocytes was decreased and the proportion of astrocytes was increased, and astrocytes and microglia showed idiopathic PD-specific cellular proliferation as well as dysregulation of genes associated with unfolded protein responses and cytokine signaling [29]. In the present study, compared to the NC group, the proportion of oligodendrocytes and astrocytes was increased in the substantia nigra of PD. These findings suggested that oligodendrocytes and astrocytes in different brain regions were not identical, and even neighboring astrocytes within the same brain region might have differences [30]. It has been reported that in PD, continuously activated glial cells by α-syn aggregates could cause chronic inflammation, thereby impairing the phagocytic activity of glia, increasing the levels of inflammatory cytokine and intercellular α- Syn spread, prompting α- Syn lesion spread [31]. Furthermore, we found that *GFAP* (astrocyte activation marker) [32], *AQP4* (densely expressed in astrocyte end-feet) [33], SERPINA3 (related to the progression of CNS diseases) [34], and *CHI3L1* (a regulator of inflammatory reactions and muscle cell proliferation) [35] were up-regulated in the PD group compared to NC group. Next, we identified three astrocyte subpopulations: Astro-C0, -C1, and -C2, and found that the Astro-C1 subpopulation was all derived from NC samples the Astro-C0 and -C2 subpopulations were associated with inflammation and apoptosis signaling pathways. In PD, the levels of inflammatory cytokines, including TNF-α, IL-2, IL-4, IL-6, and IL-1β were found to be increased [36,37]. In addition, activated (reactive) astrocytes could release a variety of chemokines and cytokines such as TNF-α and IL-1β, which are neurotoxic [38,39]. Given the Astro-C0 and -C2 subpopulations were correlated with inflammation in PD, we hypothesized that two astrocyte subpopulations might be in an activated state in PD, which was confirmed by trajectory analysis. The Astro-C1 subpopulation clustered at the front end of the differentiation trajectory, followed by a slow activation into Astro-C0, and Astro-C2 subpopulations.

Moreover, we found that *CHI3L1* was highly correlated with astrocyte activation trajectories and it was lowly expressed in the Astro-C1 and Astro-C2 subpopulations and highly expressed in the Astro-C0. *CHI3L1* is a secreted glycoprotein that plays a role in

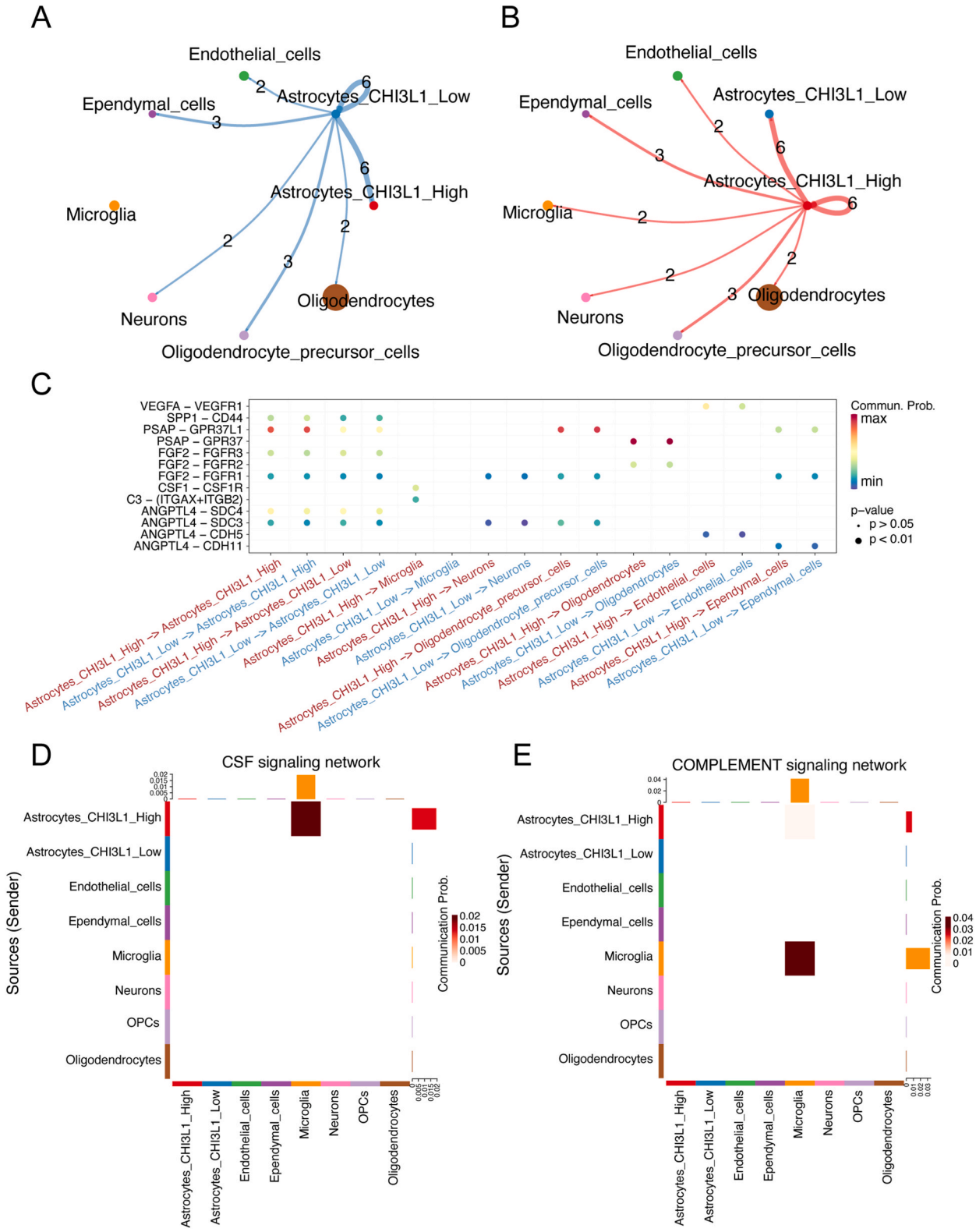

Fig. 6. *CHI3L1*^{High} astrocytes had interactions with microglia in Parkinson's disease **patients**.
A-B. The interactions among *CHI3L1*^{High}, *CHI3L1*^{Low} astrocytes, and other cells. C. The receptor-ligand pairs for interactions between *CHI3L1*^{High} or *CHI3L1*^{Low} astrocytes and other cells. D. Cell-cell interactions in the CSF signaling pathway. E. Cell-cell interactions in the COMPLEMENT signaling pathway.

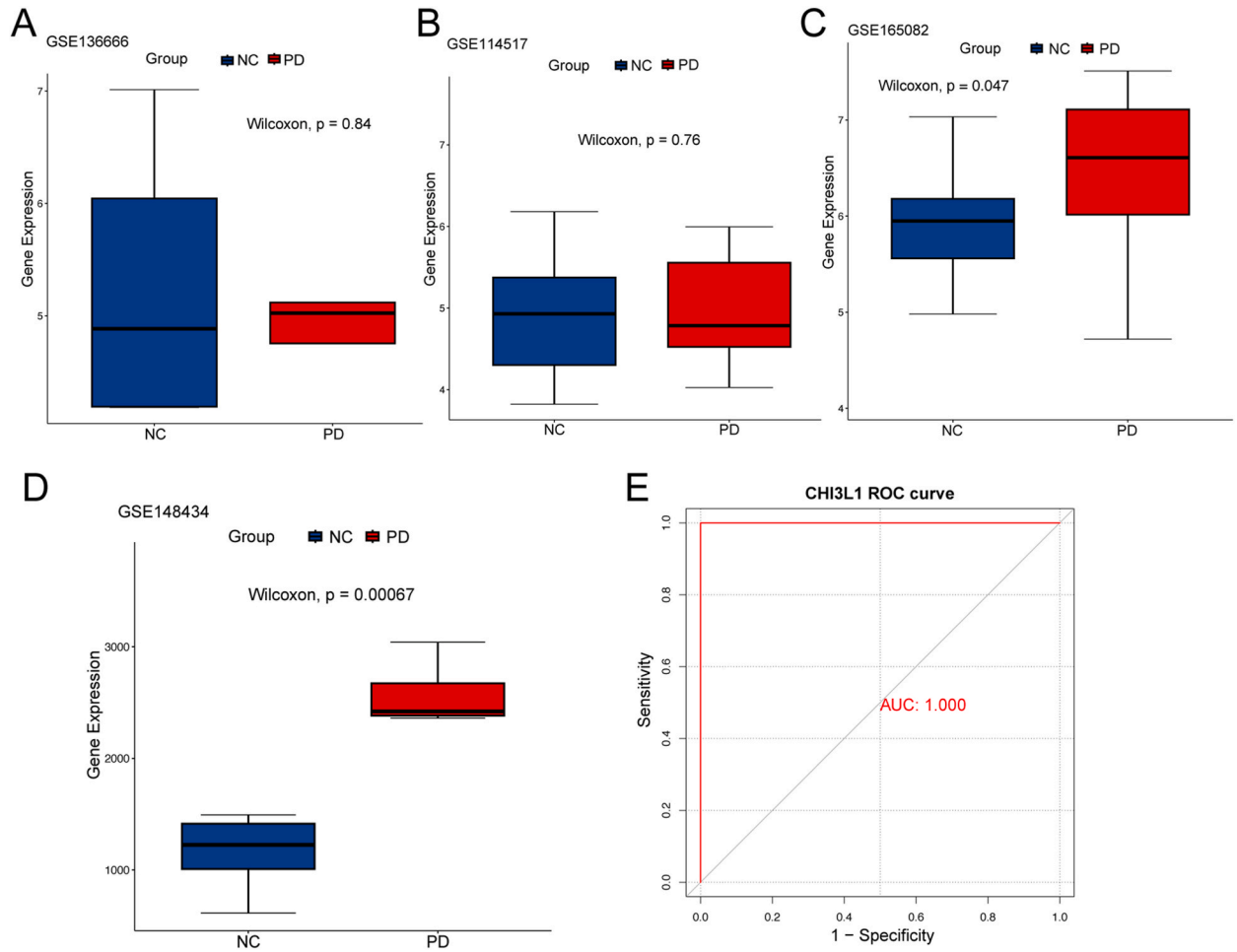

Fig. 7. *CHI3L1* might be a marker for pre-diagnosis of PD.
A-D. The expression of *CHI3L1* in Parkinson's disease and normal control samples in the GSE136666, GSE114517, GSE165082 and GSE148434 datasets. E. Diagnostic value of *CHI3L1* for Parkinson's disease in the GSE148434 dataset.

mediating inflammation, macrophage polarization, apoptosis, and carcinogenesis [40]. It has been reported that the expression of *CHI3L1* was elevated in various inflammatory diseases, including ischemic stroke [41], multiple sclerosis [42], PD [43], and Alzheimer's disease [44]. *CHI3L1* was mainly expressed and secreted by astrocytes in the brain [45], and *CHI3L1* is a powerful biomarker in neurodegenerative disease. The physiological functions of astrocyte *CHI3L1* were associated with astrocyte migration, oligodendrocyte progenitor cell (OPC) proliferation, and neural progenitor cell differentiation [46]. In the present study, we observed that *CHI3L1* expression was upregulated in PD samples from the GSE148434 dataset, demonstrating strong diagnostic potential for PD. In LPS-induced astrocytes, levels of C3, TNF-α, IL-6, and *CHI3L1* expression were found to be elevated. Furthermore, *CHI3L1* expression in astrocytes was increased by IL-1, IL-6, and TNF-α, as well as by conditioned media from M1 macrophages [47,48]. Additionally, we discovered that CHI3L1^{High} astrocytes interacted with microglia in PD patients. Microglia release inflammatory mediators such as IL-1α, IL-1β, and TNF-α, which can activate pro-inflammatory astrocytes and contribute to secondary inflammation [15,49]. CHI3L1 could bind to ACTN4 and NFKB1 and enhance the activation of the NF-κB signaling pathway by promoting the nuclear translocation of NF-κB subunits [50]. Activation of the NF-κB pathway leads to increased production of cytokines, including IL-6, MCP-1, and IL-8, as well as the release of *CHI3L1* [35]. Given that CHI3L1 was mainly secreted by astrocytes, we speculated that astrocytes activated by microglia might secrete the inflammatory signaling molecule *CHI3L1*, thereby promoting the activation of the NF-κB pathway to mediate inflammatory responses and promote the pathological progression of PD.

5. Conclusion

In conclusion, this study identified three astrocyte subpopulations (Astro-C0, -C1, and -C2) in PD based on the single-cell transcriptomic profiles and found that *CHI3L1* may be a diagnostic biomarker for PD. These findings help us to better understand the heterogeneity of astrocytes in PD and provide more reference information for exploring the diagnostic approaches for PD patients in

the future.

CRediT authorship contribution statement

Zhongying Gong: Supervision, Project administration, Funding acquisition, Formal analysis, Conceptualization. **Dan Guo:** Writing – original draft, Validation. **Yufeng Lin:** Formal analysis. **Zhiwei Liu:** Visualization, Formal analysis. **Mengdi Lv:** Visualization, Formal analysis. **Xinxin Liu:** Writing – original draft, Visualization. **Yang Yao:** Writing – original draft. **Sijia Wang:** Visualization. **Yuan Wang:** Visualization, Formal analysis. **Zhiyun Wang:** Writing – review & editing, Supervision, Project administration.

Data availability statement

The datasets presented in this study can be found in online repositories. The names of the repository/repositories and accession number(s) can be found in the article/Supplementary Material.

Consent for publication

All authors have read and approved the manuscript.

Funding information

This work was supported by a grant from the Natural Science Foundation of Tianjin, (22JCYJC00980).

Declaration of competing interest

The authors declare that they have no known competing financial interests or personal relationships that could have appeared to influence the work reported in this paper.

Appendix A. Supplementary data

Supplementary data to this article can be found online at https://doi.org/10.1016/j.heliyon.2025.e42051.

References

[1] M.T. Hayes, Parkinson's disease and parkinsonism, Am. J. Med. 132 (2019) 802–807.
[2] S.G. Reich, J.M. Savitt, Parkinson's disease, Med. Clin. 103 (2019) 337–350.
[3] O.B. Tysnes, A. Storstein, Epidemiology of Parkinson's disease, Journal of neural transmission (Vienna, Austria 124 (1996) 901–905, 2017.
[4] E. Tolosa, A. Garrido, S.W. Scholz, W. Poewe, Challenges in the diagnosis of Parkinson's disease, Lancet Neurol. 20 (2021) 385–397.
[5] T.W. Liu, C.M. Chen, K.H. Chang, Biomarker of neuroinflammation in Parkinson's disease, Int. J. Mol. Sci. 23 (2022).
[6] B. Araújo, R. Caridade-Silva, C. Soares-Guedes, J. Martins-Macedo, E.D. Gomes, S. Monteiro, F.G. Teixeira, Neuroinflammation and Parkinson's disease-from neurodegeneration to therapeutic opportunities, Cells 11 (2022).
[7] L. Guzman-Martinez, R.B. Maccioni, V. Andrade, L.P. Navarrete, M.G. Pastor, N. Ramos-Escobar, Neuroinflammation as a common feature of neurodegenerative disorders, Front. Pharmacol. 10 (2019) 1008.
[8] R. Niranjan, The role of inflammatory and oxidative stress mechanisms in the pathogenesis of Parkinson's disease: focus on astrocytes, Mol. Neurobiol. 49 (2014) 28–38.
[9] I. Miyazaki, M. Asanuma, Therapeutic strategy of targeting astrocytes for neuroprotection in Parkinson's disease, Curr. Pharmaceut. Des. 23 (2017) 4936–4947.
[10] M.E. Tremblay, M.R. Cookson, L. Civiero, Glial phagocytic clearance in Parkinson's disease, Mol. Neurodegener. 14 (2019) 16.
[11] I. Miyazaki, M. Asanuma, Neuron-astrocyte interactions in Parkinson's disease, Cells 9 (2020).
[12] T.M. Sonninen, R.H. Hämäläinen, M. Koskuvi, M. Oksanen, A. Shakirzyanova, S. Wojciechowski, K. Puttonen, N. Naumenko, G. Goldsteins, N. Laham-Karam, M. Lehtonen, P. Tavi, J. Koistinaho, Š. Lehtonen, Metabolic alterations in Parkinson's disease astrocytes, Sci. Rep. 10 (2020) 14474.
[13] H. Phatnani, T. Maniatis, Astrocytes in neurodegenerative disease, Cold Spring Harbor Perspect. Biol. 7 (2015).
[14] T.I. Kam, J.T. Hinkle, T.M. Dawson, V.L. Dawson, Microglia and astrocyte dysfunction in Parkinson's disease, Neurobiol. Dis. 144 (2020) 105028.
[15] S.A. Liddelow, K.A. Guttenplan, L.E. Clarke, F.C. Bennett, C.J. Bohlen, L. Schirmer, M.L. Bennett, A.E. Münch, W.S. Chung, T.C. Peterson, D.K. Wilton, A. Frouin, B.A. Napier, N. Panicker, M. Kumar, M.S. Buckwalter, D.H. Rowitch, V.L. Dawson, T.M. Dawson, B. Stevens, B.A. Barres, Neurotoxic reactive astrocytes are induced by activated microglia, Nature 541 (2017) 481–487.
[16] M.Y. Batiuk, A. Martirosyan, J. Wahis, F. de Vin, C. Marneffe, C. Kusserow, J. Koeppen, J.F. Viana, J.F. Oliveira, T. Voet, C.P. Ponting, T.G. Belgard, M.G. Holt, Identification of region-specific astrocyte subtypes at single cell resolution, Nat. Commun. 11 (2020) 1220.
[17] D. Lanjakornsiripan, B.J. Pior, D. Kawaguchi, S. Furutachi, T. Tahara, Y. Katsuyama, Y. Suzuki, Y. Fukazawa, Y. Gotoh, Layer-specific morphological and molecular differences in neocortical astrocytes and their dependence on neuronal layers, Nat. Commun. 9 (2018) 1623.
[18] C. Lang, K.R. Campbell, B.J. Ryan, P. Carling, M. Attar, J. Vowles, O.V. Perestenko, R. Bowden, F. Baig, M. Kasten, M.T. Hu, S.A. Cowley, C. Webber, R. Wade-Martins, Single-cell sequencing of iPSC-dopamine neurons reconstructs disease progression and identifies HDAC4 as a regulator of Parkinson cell phenotypes, Cell Stem Cell 24 (2019) 93–106.e106.
[19] H. Xu, J. Jia, Single-cell RNA sequencing of peripheral blood reveals immune cell signatures in Alzheimer's disease, Front. Immunol. 12 (2021) 645666.
[20] F.D. Ledley, H.E. Grenett, M. McGinnis-Shelnutt, S.L. Woo, Retroviral-mediated gene transfer of human phenylalanine hydroxylase into NIH 3T3 and hepatoma cells, Proc. Natl. Acad. Sci. U. S. A. 83 (1986) 409–413.
[21] S. Aibar, C.B. González-Blas, T. Moerman, V.A. Huynh-Thu, H. Imrichova, G. Hulselmans, F. Rambow, J.C. Marine, P. Geurts, J. Aerts, J. van den Oord, Z. K. Atak, J. Wouters, S. Aerts, SCENIC: single-cell regulatory network inference and clustering, Nat. Methods 14 (2017) 1083–1086.

[22] S. Jin, C.F. Guerrero-Juarez, L. Zhang, I. Chang, R. Ramos, C.H. Kuan, P. Myung, M.V. Plikus, Q. Nie, Inference and analysis of cell-cell communication using CellChat, Nat. Commun. 12 (2021) 1088.
[23] M.G. Tansey, R.L. Wallings, M.C. Houser, M.K. Herrick, C.E. Keating, V. Joers, Inflammation and immune dysfunction in Parkinson disease, Nat. Rev. Immunol. 22 (2022) 657–673.
[24] P.L. McGeer, S. Itagaki, B.E. Boyes, E.G. McGeer, Reactive microglia are positive for HLA-DR in the substantia nigra of Parkinson's and Alzheimer's disease brains, Neurology 38 (1988) 1285–1291.
[25] T. Nagatsu, M. Mogi, H. Ichinose, A. Togari, Cytokines in Parkinson's disease, J. Neural. Transm. Suppl. (2000) 143–151.
[26] M.G. Tansey, M. Romero-Ramos, Immune system responses in Parkinson's disease: early and dynamic, Eur. J. Neurosci. 49 (2019) 364–383.
[27] H. Braak, M. Sastre, K. Del Tredici, Development of alpha-synuclein immunoreactive astrocytes in the forebrain parallels stages of intraneuronal pathology in sporadic Parkinson's disease, Acta Neuropathol. 114 (2007) 231–241.
[28] L.Y. Fan, J. Yang, R.Y. Liu, Y. Kong, G.Y. Guo, Y.M. Xu, Integrating single-nucleus sequence profiling to reveal the transcriptional dynamics of Alzheimer's disease, Parkinson's disease, and multiple sclerosis, J. Transl. Med. 21 (2023) 649.
[29] S. Smajić, C.A. Prada-Medina, Z. Landoulsi, J. Ghelfi, S. Delcambre, C. Dietrich, J. Jarazo, J. Henck, S. Balachandran, S. Pachchek, C.M. Morris, P. Antony, B. Timmermann, S. Sauer, S.L. Pereira, J.C. Schwamborn, P. May, A. Grünewald, M. Spielmann, Single-cell sequencing of human midbrain reveals glial activation and a Parkinson-specific neuronal state, Brain 145 (2022) 964–978.
[30] H.Y. Zhang, Y. Wang, Y. He, T. Wang, X.H. Huang, C.M. Zhao, L. Zhang, S.W. Li, C. Wang, Y.N. Qu, X.X. Jiang, A1 astrocytes contribute to murine depression-like behavior and cognitive dysfunction, which can be alleviated by IL-10 or fluorocitrate treatment, J. Neuroinflammation 17 (2020) 200.
[31] R. Wang, H. Ren, E. Kaznacheyeva, X. Lu, G. Wang, Association of glial activation and α-synuclein pathology in Parkinson's disease, Neurosci. Bull. 39 (2023) 479–490.
[32] A. de Reus, O. Basak, W. Dykstra, J.V. van Asperen, E.J. van Bodegraven, E.M. Hol, GFAP-isoforms in the nervous system: understanding the need for diversity, Curr. Opin. Cell Biol. 87 (2024) 102340.
[33] A. Vandebroek, M. Yasui, Regulation of AQP4 in the central nervous system, Int. J. Mol. Sci. (2020) 21.
[34] C. Baker, O. Belbin, N. Kalsheker, K. Morgan, SERPINA3 (aka alpha-1-antichymotrypsin), Front. Biosci. : J. Vis. Literacy 12 (2007) 2821–2835.
[35] H. Kainulainen, CHI3L1–a novel myokine, Acta Physiol. 216 (2016) 260–261.
[36] M. Mogi, M. Harada, H. Narabayashi, H. Inagaki, M. Minami, T. Nagatsu, Interleukin (IL)-1 beta, IL-2, IL-4, IL-6 and transforming growth factor-alpha levels are elevated in ventricular cerebrospinal fluid in juvenile parkinsonism and Parkinson's disease, Neurosci. Lett. 211 (1996) 13–16.
[37] M. Mogi, M. Harada, P. Riederer, H. Narabayashi, K. Fujita, T. Nagatsu, Tumor necrosis factor-alpha (TNF-alpha) increases both in the brain and in the cerebrospinal fluid from parkinsonian patients, Neurosci. Lett. 165 (1994) 208–210.
[38] L.T. Lau, A.C. Yu, Astrocytes produce and release interleukin-1, interleukin-6, tumor necrosis factor alpha and interferon-gamma following traumatic and metabolic injury, J. Neurotrauma 18 (2001) 351–359.
[39] M.C. Leal, J.C. Casabona, M. Puntel, F.J. Pitossi, Interleukin-1β and tumor necrosis factor-α: reliable targets for protective therapies in Parkinson's Disease? Front. Cell. Neurosci. 7 (2013) 53.
[40] I.J. Yeo, C.K. Lee, S.B. Han, J. Yun, J.T. Hong, Roles of chitinase 3-like 1 in the development of cancer, neurodegenerative diseases, and inflammatory diseases, Pharmacol. Ther. 203 (2019) 107394.
[41] Q. Xu, L. Sun, Y. Wang, R. Wang, Y. Jia, D. Guo, M. Shi, P. Yang, Y. Zhang, Z. Zhu, Causal effects of YKL-40 on ischemic stroke and its subtypes: a 2-sample mendelian randomization study, J. Am. Heart Assoc. 12 (2023) e029000.
[42] I. Ahmad, S. Wergeland, E. Oveland, L. Bø, An association of chitinase-3 like-protein-1 with neuronal deterioration in multiple sclerosis, ASN Neuro 15 (2023) 17590914231198980.
[43] S. Hall, Y. Surova, A. Öhrfelt, K. Blennow, H. Zetterberg, O. Hansson, Longitudinal measurements of cerebrospinal fluid biomarkers in Parkinson's disease, Mov. Disord. : official journal of the Movement Disorder Society 31 (2016) 898–905.
[44] L. Wang, T. Gao, T. Cai, K. Li, P. Zheng, J. Liu, Cerebrospinal fluid levels of YKL-40 in prodromal Alzheimer's disease, Neurosci. Lett. 715 (2020) 134658.
[45] J. Wurm, S.P. Behringer, V.M. Ravi, K. Joseph, N. Neidert, J.P. Maier, R. Doria-Medina, M. Follo, D. Delev, D. Pfeifer, J. Beck, R. Sankowski, O. Schnell, D. H. Heiland, Astrogliosis releases pro-oncogenic chitinase 3-like 1 causing MAPK signaling in glioblastoma, Cancers 11 (2019).
[46] F. Li, A. Liu, M. Zhao, L. Luo, Astrocytic Chitinase-3-like protein 1 in neurological diseases: potential roles and future perspectives, J. Neurochem. 165 (2023) 772–790.
[47] R. Bhardwaj, J.W. Yester, S.K. Singh, D.D. Biswas, M.J. Surace, M.R. Waters, K.F. Hauser, Z. Yao, B.F. Boyce, T. Kordula, RelB/p50 complexes regulate cytokine-induced YKL-40 expression, Journal of immunology (Baltimore, Md. 194 (1950) 2862–2870, 2015.
[48] D. Bonneh-Barkay, S.J. Bissel, J. Kofler, A. Starkey, G. Wang, C.A. Wiley, Astrocyte and macrophage regulation of YKL-40 expression and cellular response in neuroinflammation, Brain Pathol. 22 (2012) 530–546.
[49] H.S. Kwon, S.H. Koh, Neuroinflammation in neurodegenerative disorders: the roles of microglia and astrocytes, Transl. Neurodegener. 9 (2020) 42.
[50] T. Zhao, J. Zeng, Y. Xu, Z. Su, Y. Chong, T. Ling, H. Xu, H. Shi, M. Zhu, Q. Mo, X. Huang, Y. Li, X. Zhang, H. Ni, Q. You, Chitinase-3 like-protein-1 promotes glioma progression via the NF-κB signaling pathway and tumor microenvironment reprogramming, Theranostics 12 (2022) 6989–7008.